# Electronic Supporting Information

## 1D Ni-Co Oxide and Sulfide Nanoarray/Carbon Aerogel Hybrid Nanostructures for Asymmetric Supercapacitors with High Energy Density and Excellent Cycle Stability

Pin Hao[a], Jian Tian[b], Yuanhua Sang[c], Chia-Chi Tuan[d], Guanwei Cui[a], Xifeng Shi[a], C.P. Wong[d], Bo Tang[a*] and Hong Liu[c*]

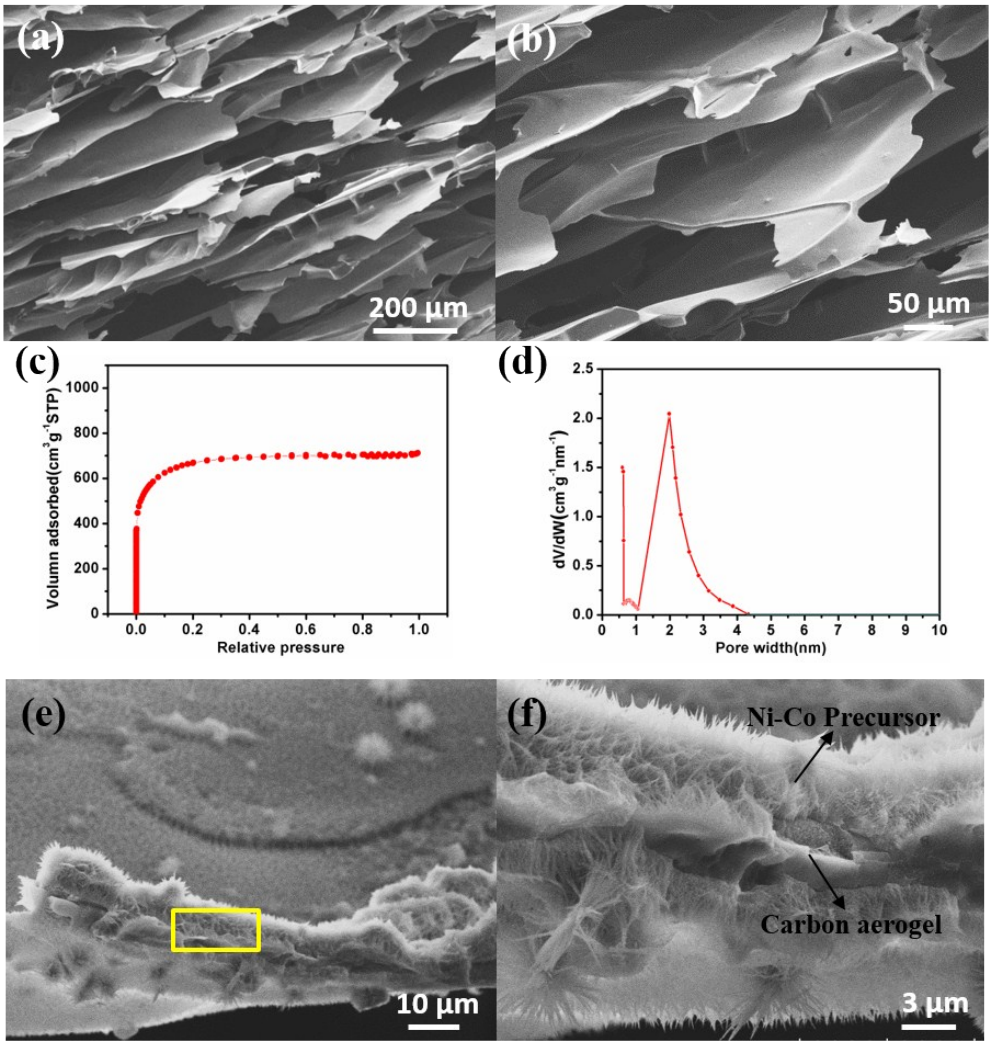


Fig.S1 (a, b) SEM images and (c, d) nitrogen adsorption/desorption isotherm and pore size distribution of carbon aerogel, (e, f) SEM images of Ni-Co precursor/carbon aerogel hybrid nanostructure

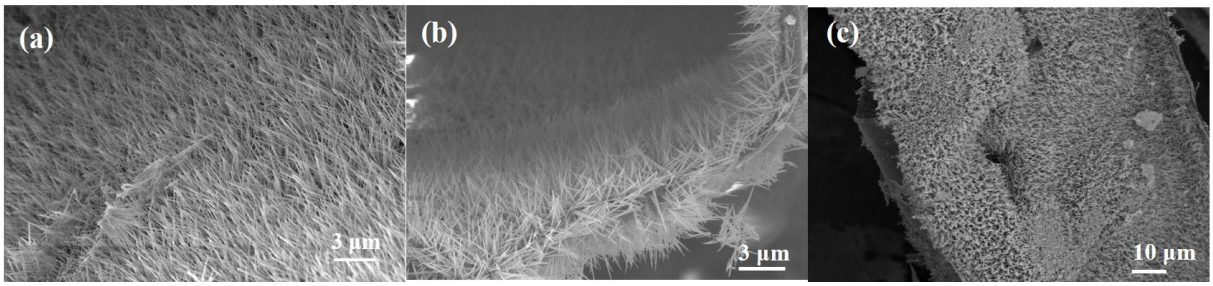


Fig.S2 SEM images of the fragment of (a) Ni-Co precursor/carbon aerogel, (b) NCOC and (c) NCSC after grind.

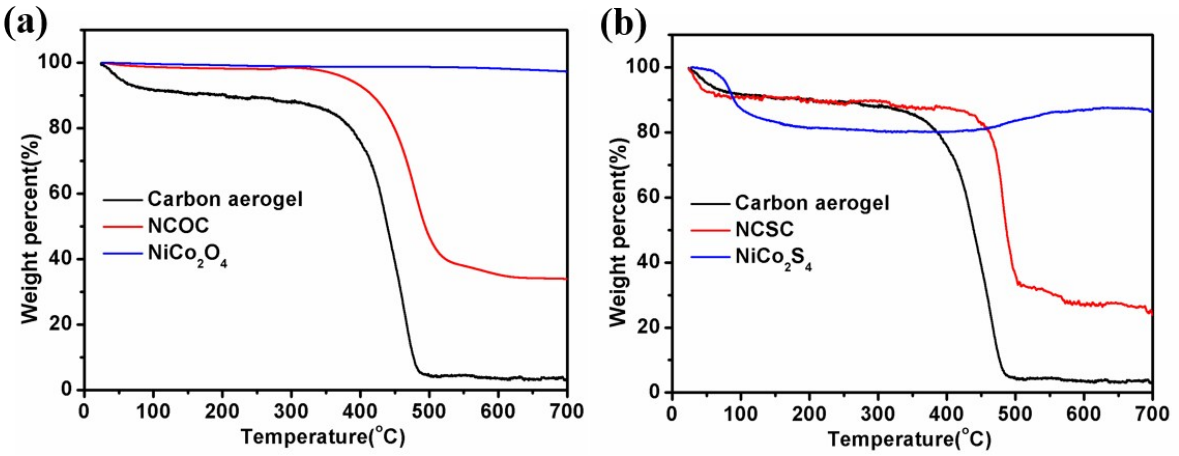


Fig.S3 TGA curves of all samples in air atmosphere from room temperature to 700 °C

In order to estimate the mass ratio of MTMCs to CA in NCOC and NCSC, the TGA analysis curves of the samples were recorded on a TA Instruments TGA Q5000 equipment in an air flowing with the heating rate of 3 °C $min^{-1}$. Fig.S3 is the obtained weight loss curves. For comparison, the TGA results for pure $NiCo_2O_4$, $NiCo_2S_4$ and CA are also shown in the figures. As shown in Fig.S3a, there is almost no weight loss for pure $NiCo_2O_4$, while the weight loss of pure CA is calculated to be 97% due to the combustion of carbon. For the sample of NCOC, there are two main weight loss steps up to 500 °C. The first step with a negligible weight loss occurs below 100 °C is corresponding to the removal of adsorbed water. The second step occurs between 100 °C and 500 °C with a weight loss of about 64.5%, indicating carbon combustion. From Fig.S3b, we can see there is a little weight increase of pure $NiCo_2S_4$ when the temperature is above 500 °C, indicating that the phase of $NiCo_2S_4$ has been changed.

However, there is no weight change below 500 °C, suggesting that $NiCo_2S_4$ is stable below 500 °C. The TGA curve of CA is basically flat and stabilized above 500 °C, confirming that the carbon combustion occurs between 100 °C and 500 °C, so we can conclude that the weight loss of NCSC between 100 °C and 500 °C is corresponding to the carbon combustion. Hence, the weight loss of NCSC about 57.7% between 100 °C and 500 °C is the mass percent of CA in the sample of NCSC. Therefore, the mass ratio of $NiCo_2O_4$ to CA in NCOC and $NiCo_2S_4$ to CA in NCSC is estimated to be 1:1.9 and 1:1.7, respectively.

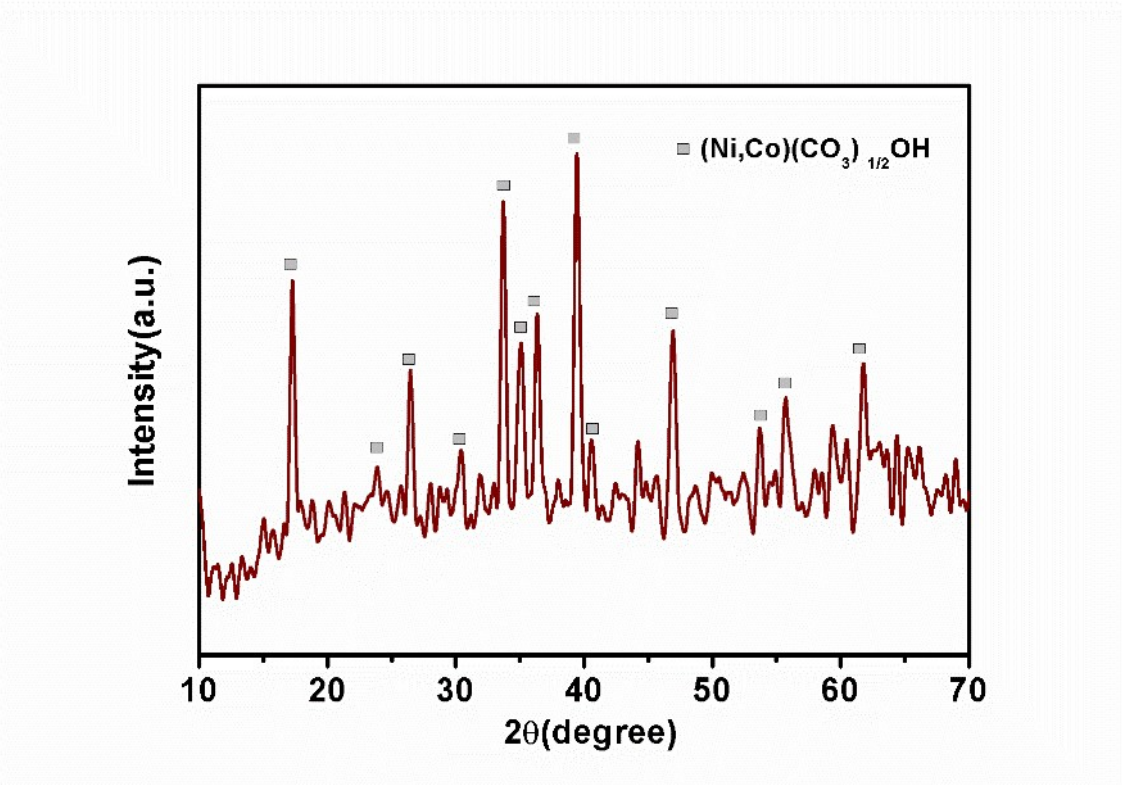


Fig.S4 XRD pattern of the Ni-Co precursor nanoneedles/carbon aerogel

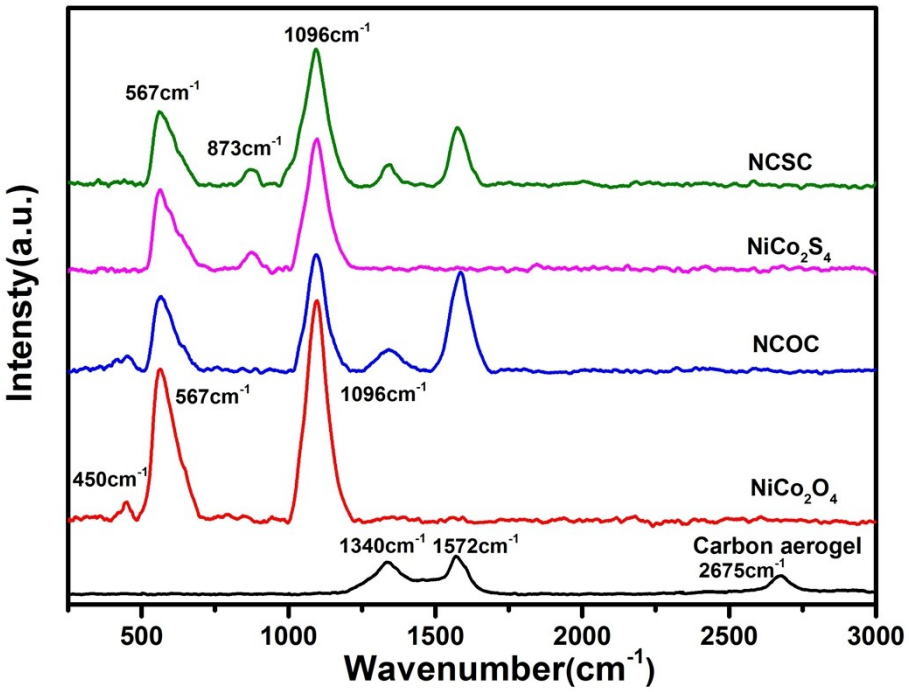


Fig.S5 Raman spectra of samples

Fig.S5 shows the raman spectra of the samples. The typical vibrational bands of carbon aerogels can be found at 1340 $cm^{-1}$, 1572 $cm^{-1}$ and 2675 $cm^{-1}$, corresponding to the D band, the G band and 2D band, respectively. The pure $NiCo_2O_4$ nanoneedles show three strong peaks at around 450, 567, and 1096 $cm^{-1}$, which are attributed to the intrinsic peaks of $NiCo_2O_4$. And the pure $NiCo_2S_4$ nanotubes also display three intrinsic peaks at around 567, 873, and 1096 $cm^{-1}$. All the peaks of $NiCo_2O_4$ nanoneedles and $NiCo_2S_4$ nanotubes can be found in the spectra of NCOC and NCSC, respectively, further indicating the formation of $NiCo_2O_4$ and $NiCo_2S_4$ on the carbon aerogel.

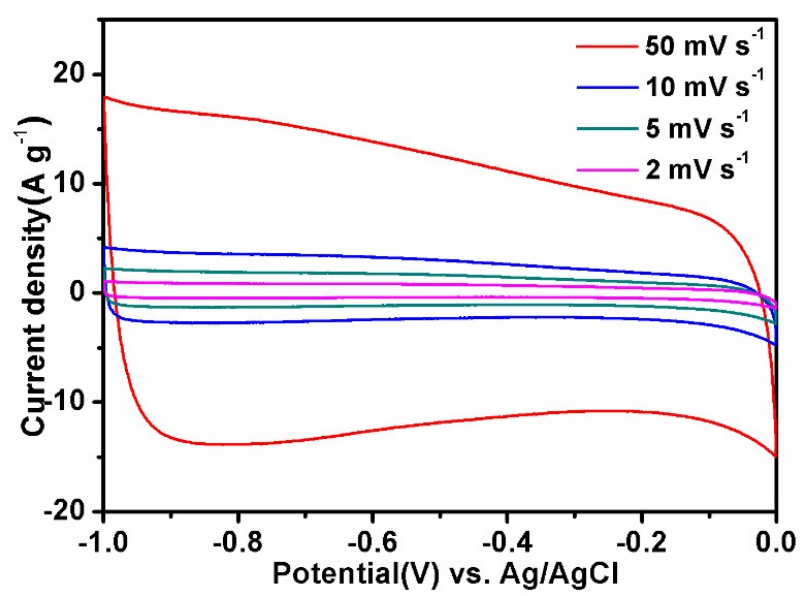


Fig.S6 CV curves of CA at different scan rates in the alkaline electrolyte

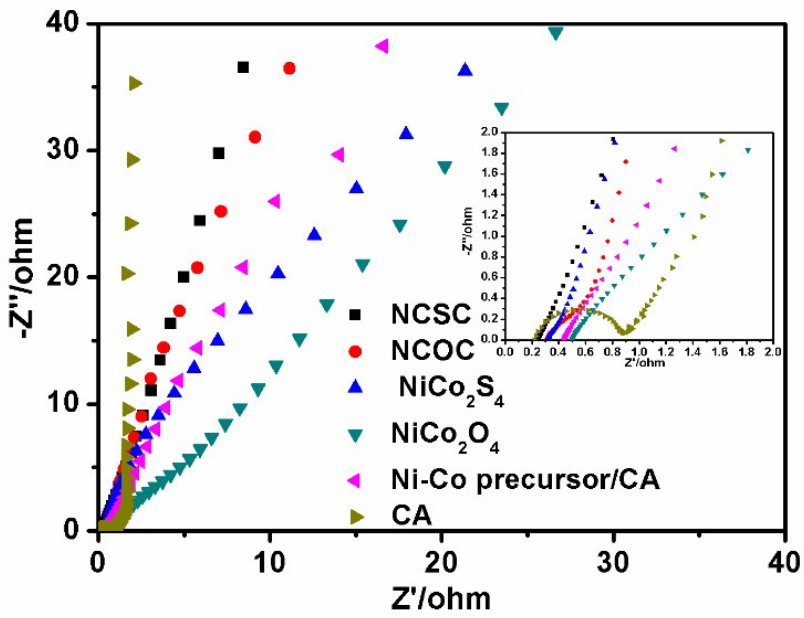


Fig.S7 Nyqusit plots of the samples. The inset image shows the magnified image of the Nyquist plot in high-frequency region, showing equivalent series resistance in high frequency region and charge transfer resistance in medium frequency region

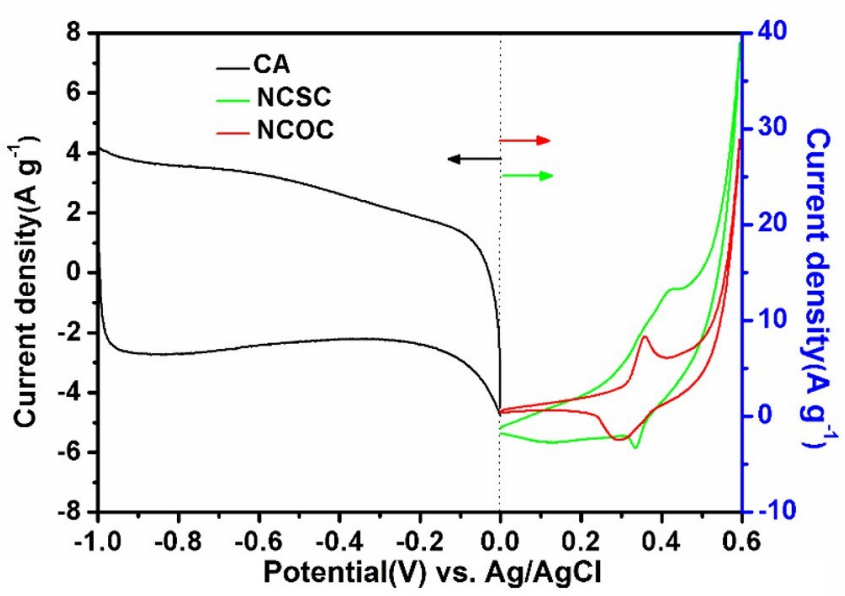


Fig.S8 CV curves of CA, NCOC and NCSC electrodes performed in a three-electrode cell in a 2 M KOH solution at a scan rate of 10 mV $s^{-1}$

Tab.S1 Comparison of electrochemical performance for our samples with other Ni-Co complex compound materials based asymmetric supercapacitors

| Asymmetric supercapacitors | Energy density (Wh $kg^{-1}$) | Power density (W $kg^{-1}$) | Cycle stability | Ref. |
|---|---|---|---|---|
| NCSC//CA(in this work) | 55.3 | 400 | 5000 cycles 96.4% | -- |
| NCOC//CA(in this work) | 47.5 | 400 | 5000 cycles 92% | -- |
| $NiCo_2S_4$ nanosheet/NCF//OMC/NCF | 45.5 | 512 | 10000 cycles 70.4% | 35 |
| Mesoporous $NiCo_2S_4$ Nanosheets//AC | 25.5 | 334 | 4000 cycles 85.6% | 54 |
| $NiCo_2O_4$//AC | 14.7 | 175 | 5000 cycles 85 % | 28 |
| $NiCo_2S_4$ nanotube/Ni//RGO | 31.5 | 156.6 | -- | 55 |
| $NiCo_2O_4$/RGO composite//AC | 23.3 | 324.9 | 2500 cycles 83% | 56 |
| $Ni_xCo_{1-x}$ LDH/ZTO //AC | 23.7 | 284.2 | 5000 cycles 92.7% | 32 |
| $NiCo_2S_4$// graphene/CS | 42.3 | 476 | 10000 cycles 78.6% | 27 |
| $CoMoO_4$-$NiMoO_4 \cdot xH_2O$ bundles//AC | 24.95 | 164.5 | 1000 cycles <85% | 57 |

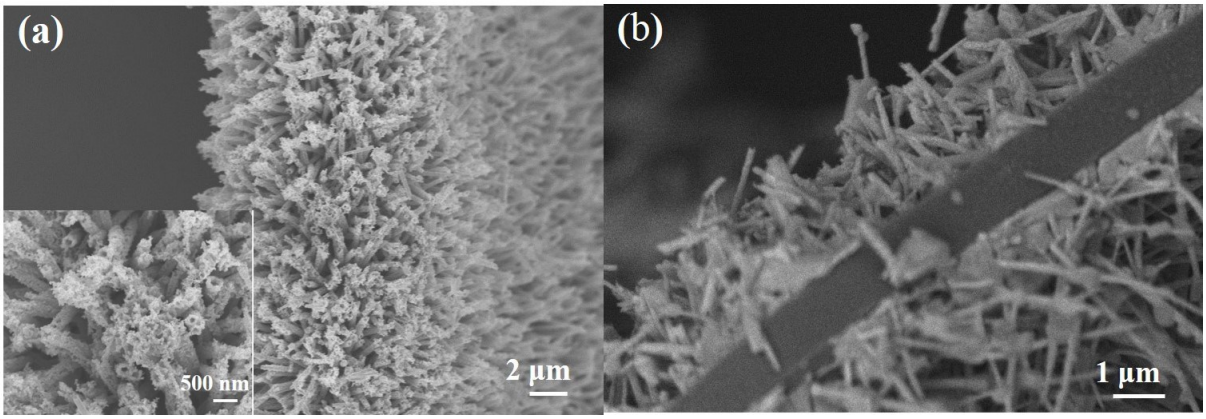


Fig.S9 SEM images of (a) NCSC and (b) NCOC electrode after the cycling test. Inset in (a) is magnified image of (a).

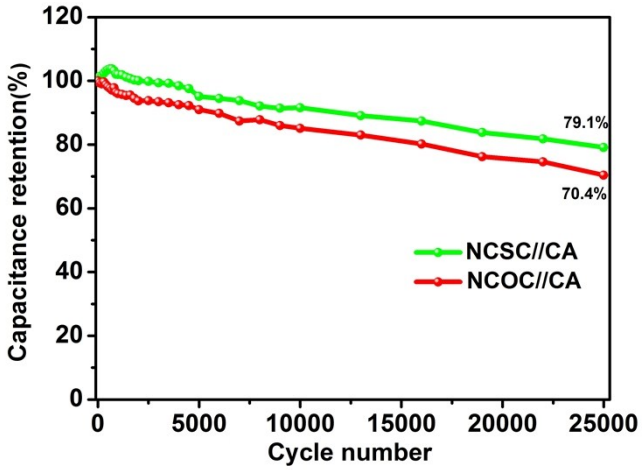


Fig.S10 Cycling performance of NCSC//CA and NCOC//CA at 6 A $g^{-1}$ over 25000 cycles